The EMBO Journal (2008) 27, 2943–2954 | © 2008 European Molecular Biology Organization | All Rights Reserved 0261-4189/08
www.embojournal.org

THE EMBO JOURNAL

Clustering of VASP actively drives processive, WH2 domain-mediated actin filament elongation

Dennis Breitsprecher[1,4], Antje K Kiesewetter[1,4], Joern Linkner[1], Claus Urbanke[1], Guenter P Resch[2,3], J Victor Small[2] and Jan Faix[1,*]

[1]Institute for Biophysical Chemistry, Hannover Medical School, Hannover, Germany, [2]Institute of Molecular Biotechnology, Austrian Academy of Sciences, Vienna, Austria and [3]Research Institute of Molecular Pathology, Vienna, Austria

Vasodilator-stimulated phosphoprotein (VASP) is a key regulator of dynamic actin structures like filopodia and lamellipodia, but its precise function in their formation is controversial. Using *in vitro* TIRF microscopy, we show for the first time that both human and *Dictyostelium* VASP are directly involved in accelerating filament elongation by delivering monomeric actin to the growing barbed end. In solution, DdVASP markedly accelerated actin filament elongation in a concentration-dependent manner but was inhibited by low concentrations of capping protein (CP). In striking contrast, VASP clustered on functionalized beads switched to processive filament elongation that became insensitive even to very high concentrations of CP. Supplemented with the *in vivo* analysis of VASP mutants and an EM structure of the protein, we propose a mechanism by which membrane-associated VASP oligomers use their WH2 domains to effect both the tethering of actin filaments and their processive elongation in sites of active actin assembly.

The EMBO Journal (2008) **27,** 2943–2954. doi:10.1038/emboj.2008.211; Published online 16 October 2008
Subject Categories: cell & tissue architecture
Keywords: actin assembly; capping protein; Ena/VASP proteins; processivity; TIRF microscopy

Introduction

Enabled/vasodilator-stimulated phosphoproteins (Ena/VASP) are a structurally conserved family found in vertebrates, invertebrates and *Dictyostelium discoideum* cells. All members of the family share a conserved domain architecture: an N-terminal EVH1 domain required for subcellular localization followed by a central proline-rich region (PRD), and finally a C-terminal EVH2 domain mediating interactions with actin as well as the multimerization of the molecule. Vertebrates express three Ena-related proteins Mena, EVL and VASP, which were shown to localize to sites of active actin assembly, including focal adhesions, stress fibers, the lamellipodial leading edge and filopodial tips (Reinhard *et al*, 1992; Gertler *et al*, 1996; Rottner *et al*, 1999; Svitkina *et al*, 2003). Filopodia fail to form in *Dictyostelium* cells lacking the single VASP member and are markedly reduced in neuronal cells lacking all three Ena/VASP proteins, consistent with a conserved requirement of this protein family in filopodia formation in evolutionary distant organisms (Han *et al*, 2002; Schirenbeck *et al*, 2006; Dent *et al*, 2007; Kwiatkowski *et al*, 2007). Moreover, an increase or decrease in the levels of Ena/VASP proteins has been reported to lead to respectively longer or shorter filaments in lamellipodia (Bear *et al*, 2002). Despite the relevance of Ena/VASP proteins for many actin-based processes such as cell migration, cell adhesion and the intracellular movement of pathogens such as *Listeria* (Laurent *et al*, 1999), their exact molecular function is still not clearly understood. A polyproline motif within the surface protein ActA of *Listeria* was previously identified to mediate recruitment of Ena/VASP proteins by binding to their EVH1 domains and to enhance the intra- and intercellular actin-based motility of this pathogen (Niebuhr *et al*, 1997). Homologous polyproline repeats containing the consensus motif FP_4 in zyxin and vinculin were also shown to be involved in the subcellular targeting of Ena/VASP proteins to focal adhesions (Reinhard *et al*, 1995b; Brindle *et al*, 1996). Although additional EVH1-binding motifs were subsequently identified, it is currently unclear which interaction partners recruit Ena/VASP proteins to filopodia tips. Among the potential candidates are lamellipodin/Mig-10 (Krause *et al*, 2004) and the related protein PREL1/RIAM (Lafuente *et al*, 2004; Jenzora *et al*, 2005).

Ena/VASP proteins tetramerize, bind directly to both monomeric and filamentous actin and were shown to nucleate and bundle actin filaments *in vitro* (Laurent *et al*, 1999). A recent study suggested that filament bundling is also required *in vivo*, as a DdVASP mutant lacking the F-actin binding site failed to rescue filopodium formation in *Dictyostelium* DdVASP-null cells (Schirenbeck *et al*, 2006). Other potential links between Ena/VASP proteins and actin dynamics involve their ability to bind to the actin monomer-binding protein profilin and profilin–actin complexes through their central proline-rich domain (Ferron *et al*, 2007; Kursula *et al*, 2008). Recent structural data indicate that actin from profilin–actin complexes can be directly transferred to the G-actin binding (GAB) domain for filament elongation (Ferron *et al*, 2007). Although other studies also hypothesized that Ena/VASP members might be directly implicated in filament elongation, this has actually never been demonstrated. Very recently, Pasic *et al* (2008) observed barbed-end capture of single filaments, but found no acceleration of filament assembly by murine VASP. Conflicting results were reported concerning the ability of VASP to compete with heterodimeric capping protein (CP). Whereas some studies indicated that VASP antagonizes filament capping by CP to promote spontaneous

*Corresponding author. Department of Biophysical Chemistry, Hannover Medical School, OE4350, Carl-Neuberg-Strasse 1, Hannover D-30623, Germany. Tel.: +49 511 532 2928; Fax: +49 511 532 5966; E-mail: faix@bpc.mh-hannover.de
[4]These authors contributed equally to this work

Received: 19 May 2008; accepted: 17 September 2008; published online: 16 October 2008

filament elongation (Bear *et al*, 2002; Barzik *et al*, 2005; Pasic *et al*, 2008), others suggested that although VASP opposes the effect of CP, it does not compete with CP for binding to barbed ends and does not protect filament barbed ends from disassembly in depolymerization assays (Samarin *et al*, 2003; Schirenbeck *et al*, 2006). A very recent review by Trichet *et al* (2008) summarizes the controversy concerning the mode of action of Ena/VASP proteins. To shed light on this issue, we have analysed actin polymerization in the presence of VASP at the single filament level using TIRF microscopy.

Results

VASP promotes actin filament elongation in a concentration-dependent manner

To characterize VASP-mediated actin assembly in detail, we used time-lapse *in vitro* TIRF microscopy on growing actin filaments. The elongation rates for the spontaneous assembly of actin using 1 μM unlabelled actin and 0.3 μM labelled actin were 10.5 ± 0.9 subunits per second for the barbed ends in our experimental setup (Figure 1B and C, Supplementary Movie 1). We then compared actin assembly in the presence of either *Dictyostelium* (DdVASP) or human VASP (hVASP) that both share the characteristic tripartite domain architecture of all Ena/VASP proteins (Figure 1A). DdVASP induced not only bundling of filaments (Figure 1B), but markedly accelerated the growth of newly formed filaments in a concentration-dependent manner, reaching a maximum at concentrations around 200 nM with 73.9 ± 7.3 subunits per second (Supplementary Movie 2). This indicated that DdVASP delivers actin monomers exclusively to the barbed ends of growing filaments in a non-processive manner (Figure 1C, Supplementary Figure 1, Supplementary Movie 3). To further investigate the mechanism of VASP-mediated actin assembly, we used a setup comparable with the one applied previously by Kovar and Pollard (2004) to demonstrate processive filament elongation by formins, and coated the coverslips with low nM amounts of DdVASP. Processive elongation of actin by coverslip-bound molecules is reflected by the growth and buckling of single actin filaments from surface foci (Kovar and Pollard, 2004). Consistent with a previous study, in which 100 nM of murine VASP were used (Pasic *et al*, 2008), we observed frequent capturing of growing barbed ends using 70 nM DdVASP, but neither a change of the growth rate nor filament buckling (Supplementary Figure 2A–C, Supplementary Movie 4). Interestingly, coating of the coverslips with 20 times more DdVASP (1.4 μM) resulted in an acceleration of filament growth but still did not produce filament buckles (Supplementary Figure 2D, Supplementary Movie 5), suggesting that DdVASP binds the barbed end, delivers actin subunits and subsequently stays attached to the side of the filament (Supplementary Figure 2E). Together, this

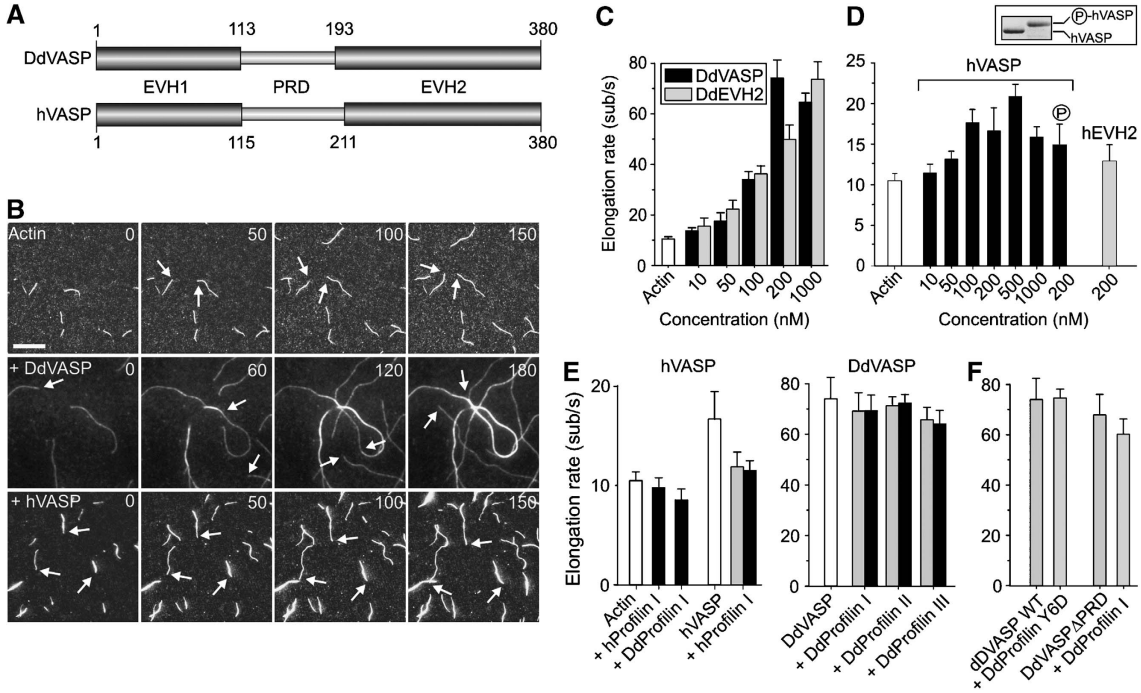

Figure 1 Analysis of VASP-mediated actin assembly by TIRF microscopy. (**A**) *D. discoideum* DdVASP and human hVASP share a similar domain organization encompassing an N-terminal EVH1, a central proline-rich region (PRD) and C-terminal EVH2 domain. Numbers indicate amino-acid residues. (**B**) VASP accelerates actin assembly *in vitro*. A concentration of 1 μM ATP-actin and 0.3 μM Alexa-Fluor-488 labelled ATP-actin (from now on referred to as 488 actin) was polymerized in the presence or absence of either 200 nM DdVASP or 200 nM hVASP on NEM-myosin II-coated glass slides in 1 × TIRF buffer containing 10 mM imidazole, 50 mM KCl, 1 mM $MgCl_2$, 1 mM EGTA, 0.2 mM ATP, 50 mM DTT, 15 mM glucose, 20 μg/ml catalase, 100 μg/ml glucose oxidase and 0.5% methylcellulose (4000 cP), pH 7.4. Time-lapse micrographs of the assembly reaction are shown. The time is indicated in seconds on top. Arrows mark barbed ends during filament elongation. Scale bar, 10 μm. (**C**) Concentration dependence of the elongation rates of DdVASP-mediated actin assembly by the full-length protein and the EVH2 domain (DdEVH2). (**D**) Comparison of the actin filament elongation rates in the presence of untreated or PKA phosphorylated WT hVASP and the hEVH2 domain alone. Inset shows SDS–PAGE of Coomassie Blue-stained non-phosphorylated and PKA-phosphorylated hVASP. (**E**) Profilin does not accelerate VASP-mediated actin assembly. The elongation rates of actin and either 200 nM hVASP (left) or 200 nM DdVASP (right) in the presence of 2 μM (grey bars) or 5 μM (black bars) of the indicated profilin isoforms are shown. (**F**) Profilin–PRD interaction is not required for VASP-mediated filament elongation. The elongation rate of 200 nM DdVASP was not affected by addition of 5 μM profilin Y6D mutant. Data in C–F correspond to means ± s.e.m.

indicates that the mechanism of VASP-mediated actin assembly is entirely different from the one exerted by formins, which remain bound to the barbed end as the filament elongates (Kovar *et al*, 2006).

hVASP bundled filaments in a parallel or anti-parallel orientation as DdVASP (Supplementary Figure 3); however, it had a less prominent effect on filament elongation, accelerating filament growth only two-fold (Figure 1B and D, Supplementary Movie 6). As previous studies indicated that mammalian VASP (mVASP) is regulated by phosphorylation (Lambrechts *et al*, 2000), we also analysed PKA-treated recombinant hVASP. Although hVASP could be entirely converted into its phosphorylated form as assessed by SDS–PAGE, no effects were observed on filament bundling or elongation (Figure 1D, Supplementary Figure 3A).

DdEVH2 alone induced virtually identical maximal actin elongation rates as full-length DdVASP (73.6 ± 7.3 subunits per second at 1 μM; Figure 1C). Similar results were obtained for the hEVH2 domain (Figure 1D). Taken together, these findings confirm that the EVH2 domain of VASP harbours all motifs required for promoting actin assembly.

VASP-mediated actin assembly in vitro is not affected by profilin

Proline-rich regions, such as the formin-homology domain-1 (FH1), have been shown to have an important function in the recruitment of profilin–actin complexes for formin-mediated filament elongation (Watanabe *et al*, 1997; Kovar *et al*, 2006). The recent co-crystallization of mammalian profilin and of the profilin–actin complex with peptides derived from the PRD of mVASP suggested an important function of this region in delivery of actin monomer to the GAB domain (Ferron *et al*, 2007; Kursula *et al*, 2008). However, neither human nor *Dictyostelium* profilin stimulated VASP-mediated filament elongation in our TIRF assay (Figure 1E). Additionally, we analysed whether abrogation of profilin recruitment to the PRD impairs actin monomer addition. This was achieved by using either a profilin mutant (Y6D) defective in binding to poly-L-proline or a DdVASP mutant lacking the PRD (DdVASPΔPRD). The mutant Y6D did not significantly lower the elongation rate, indicating that PRD–profilin interaction is not required. Consistent results were obtained with DdVASPΔPRD that was indistinguishable from WT (WT) in the presence or absence of profilin (Figure 1F).

GAB and FAB domains both contribute to filament barbed-end elongation

Owing to its higher activity in our assays, we chose DdVASP to determine the contributions of the GAB, the FAB and the Tet (tetramerization) motifs located within the EVH2 domain to filament assembly (Figure 2A). Surprisingly, mutant DdVASPΔGAB retained virtually the same activity as the WT protein (Figure 2B and C). This finding suggested that another region within the EVH2 domain, presumably the FAB motif, was also capable of recruiting actin monomers for filament elongation, as this motif, similar to GAB, displays close sequence relationship to the actin-monomer recruiting WH2 domain (Paunola *et al*, 2002; Ferron *et al*, 2007).

As hypothesized, mutant DdVASPΔFAB was also able to promote actin assembly (Figure 2B and C). It accelerated filament elongation up to 60 subunits per second already at 50 nM and reached a slightly higher maximal rate than WT (Figure 2B and C), but that dropped to 34 subunits per second at 1 μM. In agreement with previous studies (Laurent *et al*, 1999; Schirenbeck *et al*, 2006), DdVASPΔFAB did not induce any bundle formation (Figure 2B). Mutant DdVASPΔGAB/FAB lacking both actin-binding motifs was entirely inactive in filament assembly (Figure 2C). Interestingly, the maximal filament elongation rate of monomeric mutant DdVASPΔTet was drastically reduced as compared with WT or other mutants (18.3 ± 1.6 subunits per second), suggesting that the actin-binding sites within the VASP tetramer cooperate in G-actin delivery during filament assembly in solution (Figure 2B and C). Collectively, these data demonstrate that one of the two WH2-like motifs and the tetramerization domain are required for maximal polymerization rates.

To show that the FAB motif is involved in side binding of filaments, we examined actin filaments formed in the presence of DdVASP or DdVASP mutants lacking the GAB, FAB or the Tet motifs on coverslips coated with NEM-myosin II (Figure 2D–G). After antibody labelling of VASP and phalloidin staining of filamentous actin, the specimens were analysed by confocal microscopy. DdVASP and mutant DdVASPΔGAB induced the formation of prominent bundles that were decorated by the antibodies (Figure 2D and E). In contrast, mutants DdVASPΔFAB and DdVASPΔTet failed to induce bundles, and the filaments formed were not labelled for VASP (data not shown). Even when bundle formation was induced independently of VASP by the addition of poly-L-lysine, the actin bundles were not decorated by these mutants, illustrating that only tetrameric VASP containing the FAB motif displays prominent filament side binding (Figure 2F and G). Similar results were also obtained with hVASP and derived mutants (data not shown) and are consistent with previous results from sedimentation assays showing that interactions with F-actin are enhanced by VASP tetramerization (Bachmann *et al*, 1999).

VASP fails to continuously elongate filaments in the presence of CP in solution

To test how CP affects VASP-mediated actin assembly, we first determined the total cellular concentrations of DdVASP and *Dictyostelium* CP Cap32/34 by titrating total cell lysates of 2×10^5 cells with defined amounts of recombinant proteins in western blots using specific antibodies. We obtained *in vivo* values of 2 μM for DdVASP and 0.4 μM for Cap32/34 (data not shown). As both proteins share a common subcellular localization at the leading edge (Lai *et al*, 2008), it was reasonable to assume that this molar ratio of approximately 5:1 also resembles the local cellular ratio. When this concentration ratio was applied in our TIRF assay, both Cap32/34 and human CapZ inhibited actin filament elongation by DdVASP or hVASP, resulting in an average filament length of ~ 3 μm after 10 min of polymerization (Figure 3A and D). In the absence of CP, the average filament length after 10 min was 120 μm for DdVASP and 23 μm for hVASP (Figure 3B and E). Even at a ratio of 20:1 (200 nM VASP and 10 nM CP), the amount of CP was still sufficient to cap all actin filaments formed in the presence of DdVASP or hVASP. The filaments assembled in the presence of VASP were significantly longer than the actin control. Calculation of the time to growth arrest in the presence or absence of CP revealed that this effect is largely due to the enhanced filament elongation by VASP (Figure 3C and F). Taken together, these data demonstrate

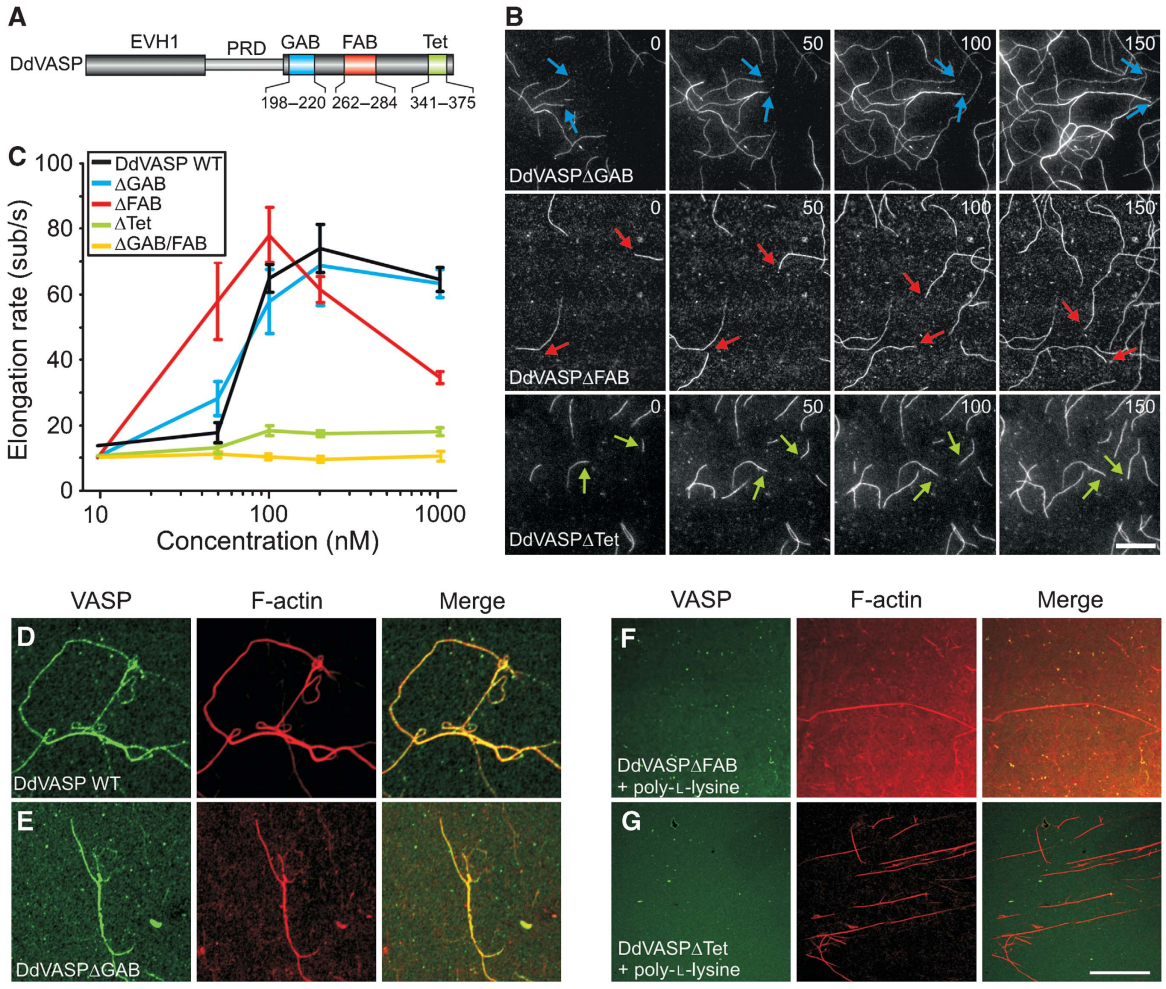

Figure 2 Analysis of DdVASP mutants lacking functional domains. (**A**) Localization of the GAB, FAB and Tet motifs within the EVH2 domain of DdVASP. Numbers indicate deleted amino-acid residues in the mutants. Mutant DdVASPΔGAB/FAB lacks residues 198–220 and 262–284. (**B**) Both WH2 domain-like actin-binding motifs can contribute to actin assembly. Time-lapse micrographs of the assembly of 1 μM ATP-actin and 0.3 μM 488 actin in 1 × TIRF buffer in the presence of 200 nM DdVASPΔGAB (blue arrows), DdVASPΔFAB (red arrows) and DdVASPΔTet (green arrows). Time and scale as in Figure 1B. (**C**) Comparison of the actin filament elongation rates in the presence of different DdVASP mutants at the concentrations indicated. The assembly rates for untagged or GST-tagged DdVASPΔTet constructs were virtually identical. Data correspond to means ± s.e.m. (**D–G**) The FAB motif and tetramerization of VASP are required for robust filament side binding. A concentration of 2 μM actin was polymerized in 1 × TIRF buffer lacking methylcellulose on glass slides coated with NEM-myosin II in the presence of 1 μM of the GST-tagged DdVASP WT, ΔGAB, ΔFAB constructs and of untagged monomeric ΔTet mutant. After 20 min, the samples were fixed and stained with anti-GST or DdVASP polyclonal antibodies. Primary antibodies were visualized with Alexa-Fluor-488-conjugated goat-anti-rabbit antibodies and F-actin was stained with rhodamine-phalloidin. Confocal images of the specimens are shown. As DdVASPΔFAB and DdVASPΔTet mutants lacked bundling activity, filament bundling was induced by 10 μM poly-L-lysine (F, G).

that, at physiological concentration ratios, VASP cannot continuously promote actin assembly in the presence of CP in solution, as it is not permanently associated with the growing barbed end.

Clustering of VASP allows processive filament elongation on functionalized beads

To mimic VASP-mediated actin assembly in a more physiological context, we coated 2-μm-diameter polystyrene beads with DdVASP, hVASP or the derived mutants to simulate actin assembly on a surface. The beads were placed in flow cells together with actin monomers in polymerization buffer and analysed by TIRF microscopy. The fluorescence of VASP-coated beads increased due to the accumulation of actin, and subsequently filaments started to grow from their surfaces. On the basis of their growth rates, two populations of filaments were identified (Figure 4A and B). One population grew at a rate corresponding to the actin control at 10.5 ± 0.9 subunits per second, whereas the other grew at significantly higher elongation rates (>60 subunits per second), indicating that these filaments were assembled by VASP and associated with their barbed ends to the bead. This is further supported by the facts that fluorescence intensity of these filaments was brightest at the bead surface (Supplementary Figure 4A) as well as by the buckling of these filaments during growth (Figure 4A–C, Supplementary Movie 7), which was never seen for coverslip-bound VASP. Buckle formation is triggered by any resistance to elongation of an actin filament growing with its barbed end attached to a fixed point (Kovar and Pollard, 2004). Additionally, VASP-coated beads captured and subsequently elongated freely growing filament barbed ends, corroborating the view that

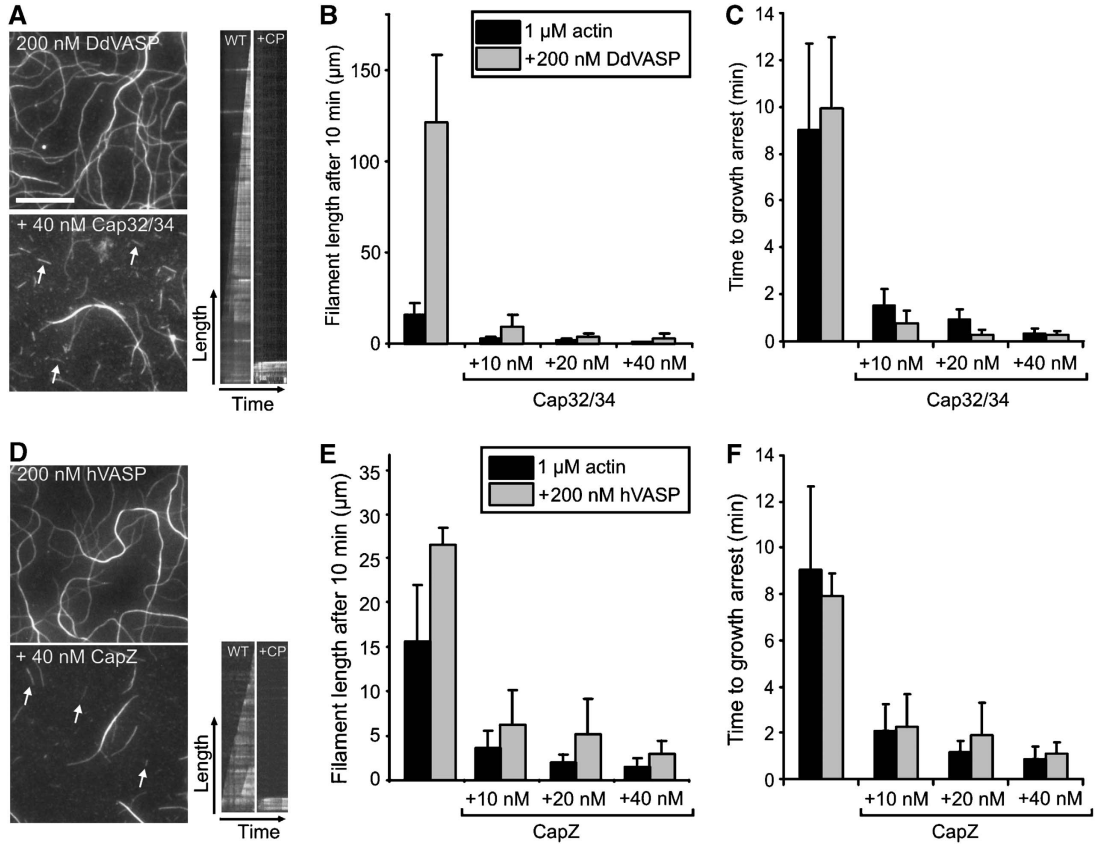

Figure 3 Capping protein inhibits VASP-mediated actin assembly in solution. (**A**, **D**) TIRF images of actin filaments polymerized for 10 min with either DdVASP or hVASP (200 nM each) in the presence and absence of Cap32/34 or CapZ (40 nM each) in 1 × TIRF buffer, respectively. White arrows in the TIRF images (left) and corresponding kymographs (right) indicate filaments that stopped growing in the presence of CP. The growth of non-capped filaments is shown for comparison. Scale bar, 10 μm. (**B**, **E**) Cap32/34 and CapZ decrease the average length of actin filaments formed in the presence of DdVASP or hVASP. Filaments formed in the presence of VASP were longer than the actin control. (**C**, **F**) The time to growth arrest is virtually independent of VASP. The times of filament elongation until capping were calculated from the elongation rates of VASP-mediated actin assembly. The lengths of at least 150 filaments for each condition were measured. Note different scales in B and E. Data correspond to means ± s.e.m.

VASP exclusively elongates barbed ends (Supplementary Figure 4B and C). Processive filament elongation was observed also on beads coated with DdVASPΔGAB, DdVASPΔFAB and, surprisingly, even on beads coated with mutant DdVASPΔTet (Figure 4C, Supplementary Movie 8), the last of which was almost inactive in solution. Consistent with the lack of one G-actin binding site, beads coated with DdVASPΔFAB and DdVASPΔGAB showed a ~2-fold slower increase in the fluorescence intensity of the beads compared with WT and ΔTet (Supplementary Figure 5, Supplementary Movie 9), whereas only mutant ΔGAB produced less buckling filaments (Figure 4D). Although beads coated with mutant DdVASPΔGAB/FAB did not accumulate actin, nucleate filaments or produce filament buckles, they were still able to capture actin filaments (Figure 4C and D, Supplementary Figures 4D and 5C). Consistent with a recent study using murine VASP (Pasic *et al*, 2008), nM amounts of mutant DdVASPΔGAB/FAB also captured filaments when coated on coverslips (Supplementary Figure 2G), indicative of the presence of an additional F-actin-binding site in the C-terminal region of VASP. The latter finding explains why DdVASPΔFAB-coated beads still produced surface-attached filaments growing with their barbed end away from the beads (Figure 4C, blue arrow). hVASP-coated beads also produced buckling filaments; however, due to the lower acceleration of actin assembly by hVASP, the elongation rates of both filament species were similar (data not shown).

Profilin had no detectable effects on actin assembly from VASP-coated beads (data not shown). To determine whether VASP density on the bead surface was critical for processivity, we incubated the beads with different amounts of DdVASP and found that extensive filament buckling occurred only close to or at saturation (Figure 4E). All mutant proteins adsorbed to the bead surface to the same extent as WT (data not shown). Calculation of the average distance at saturation revealed ~0.013 tetramers/nm^2, corresponding to a mean distance of about 8.5 nm between the DdVASP tetramers (Figure 4E, left). The critical distance that still allowed processive filament elongation on more than 50% of the coated beads was 12.6 nm (Figure 4E, right). Although VASP was also attached to the surface of coverslips, the coating density was apparently below the density required to allow processive assembly (Supplementary Figure 2). Upon saturation of the coverslip, observation of filament assembly was precluded due to the explosive increase of fluorescence caused by the rapid accumulation of labelled actin on the entire coverslip (data not shown).

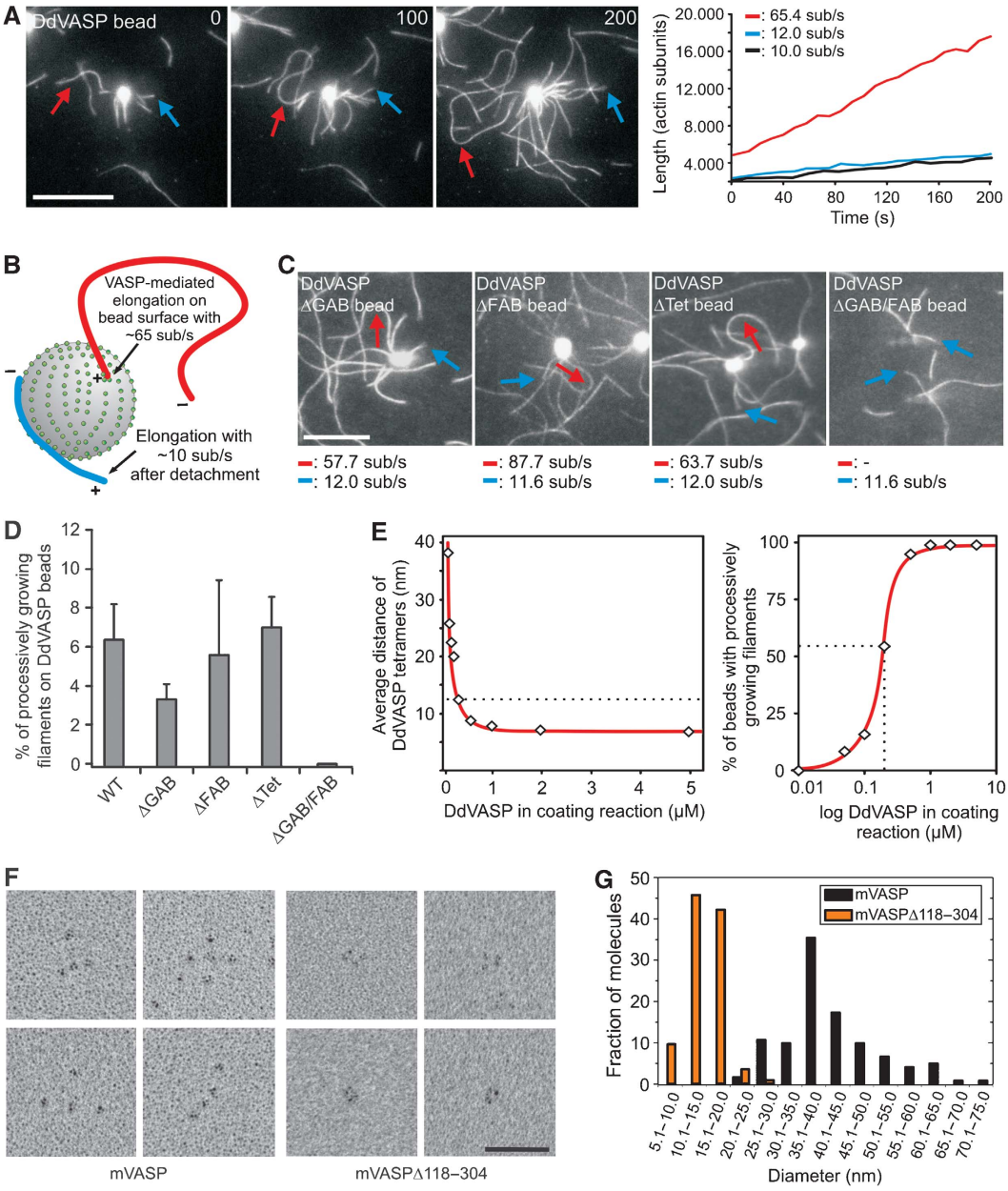

Figure 4 Clustering of VASP promotes processive actin filament elongation. (**A**) Actin assembly of 1 μM actin and 0.3 μM 488 actin in 1 × TIRF buffer on 2 μm polystyrene beads coated with the DdVASP constructs indicated. Blue arrows indicate filaments that grew with their barbed ends pointing away from the beads and red arrows highlight fast growing, buckling filaments with their barbed ends attached to the bead surface. Determination of the elongation rates (right) revealed two different filament populations. The blue and red lines correspond to the filaments marked in the time-lapse micrographs. The black line is shown as a control and corresponds to the elongation rate of a single actin filament that grew spontaneously in solution beside the beads. Time is shown in seconds. Scale bar, 10 μm. (**B**) Proposed mechanism leading to different filament populations on VASP-coated beads. + indicates a barbed and − indicates a pointed end. (**C**) Mutants DdVASPΔGAB, −ΔFAB and −ΔTet produced buckling filaments that grew with fast elongation rates, whereas DdVASPΔGAB/FAB failed to recruit actin and to assemble filaments. Scale bar and arrows are as in (A). (**D**) Quantification of the fraction of processively growing filaments on VASP-coated beads. For each box, at least 30 beads from six independent experiments were analysed. Data correspond to means per bead ± s.e.m. (**E**) Analysis of DdVASP density on functionalized polystyrene beads. Average separation distance of DdVASP tetramers on functionalized beads depends on the amount of DdVASP used for coating (left). The dashed line indicates the maximal distance at which robust processive filament elongation was observed. At the minimum concentration required for processive filament elongation, more than 50% of the beads produce buckling filaments (right). For each data point, at least 150 beads were analysed. (**F**) Electron microscopic analysis of the VASP tetramer. High magnification galleries of recombinant mVASP (left) and high magnification galleries of an mVASP deletion mutant lacking amino-acid residues 118–304 but still containing the tetramerization domain (right) are shown. Scale bars, 50 nm. (**G**) Distributions of molecular lengths of WT and mutant mVASP proteins determined from electron micrographs such as those displayed in the shown galleries in (F). The distance between the two furthermost globular domains was measured. $n = 124$ for mVASP and $n = 116$ for mutant mVASPΔ118–304.

To test whether these nearest neighbour values can be correlated with the molecular architecture of VASP, we analysed mammalian VASP by transmission electron microscopy (TEM). As shown in Figure 4F (left), the VASP molecule consists of four domains, presumably representing the N-terminal EVH1 domains encoded by the first 115 residues

(Ball *et al*, 2000). These domains are attached to each other in an exceptionally flexible manner, which was confirmed by a calculated friction ratio of 2.2 using analytical ultracentrifugation (Supplementary Figure 6). The distribution of molecular lengths between the outmost parts of the two furthermost domains revealed an average end-to-end distance of 40.9 nm and a maximal separation of more than 70 nm (Figure 4G), suggesting that most of the remaining portion of VASP harbouring PRD and EVH2 is responsible for this flexibility. To determine the minimal possible end-to-end distance between the domains, we analysed the deletion mutant mVASPΔ118–304 lacking most of the flexible region between EVH1 and the tetramerization domain. In the mutant, four tightly packed domains with an average distance of 14.4 nm and a much lower flexibility in between them were frequently visible, demonstrating that the globular domains indeed represent EVH1 (Figure 4F, right). The smallest measured distances between two adjacent EVH1 domains were in the range of 7–8 nm. As the critical distance for VASP-mediated processivity on beads is 12.6 nm, our data suggest that the VASP tetramers must be in close contact to each other to allow processive filament elongation.

Processive filament elongation prevails in the presence of CP

The switch from non-processive filament elongation in solution to processive filament elongation upon clustering on a surface was indicative of a change in the underlying mechanism and prompted us to investigate VASP-mediated actin assembly on beads in the presence of CP. Under these conditions, only filaments that were attached with their barbed ends to the beads were observed, whereas CP abolished filament growth in solution (Figure 5A and B). Most strikingly, VASP-mediated filament elongation on beads became insensitive even to very high concentrations of CP. hVASP and DdVASP still formed filaments in the presence of up to 1 μM CP (Figure 5A, Supplementary Movie 10 and 11), suggesting that VASP binding to the filament may sterically prevent access of CP to the barbed end. VASP-coated beads where unable to capture pre-capped filaments, corroborating a direct interaction of VASP with the barbed end (Supplementary Figure 4D). Next, we analysed whether DdVASP-derived mutants were impaired in filament assembly in the presence of 1 μM CP. Whereas DdVASPΔGAB and even DdVASPΔTet still allowed continuous filament elongation at a high CP concentration producing filaments longer than 20 μm within 20 min of incubation, hVASPΔFAB and DdVASPΔFAB-coated beads failed to processively elongate long filaments under these conditions (Figure 5C, Supplementary Movie 12 and 13). Instead, we observed massive detachment of short filaments with a length of maximal 4 ± 2 μm from DdVASPΔFAB-coated beads. hVASPΔFAB was incapable of producing filaments at this CP concentration. The inability of the VASPΔFAB mutants to resist higher CP concentration on beads is therefore probably due to a weaker interaction of these mutant proteins with the sides of the filament at the barbed-end region, and hence the FAB motif is critical for tight anchorage of growing filaments to the surface in the presence of CP.

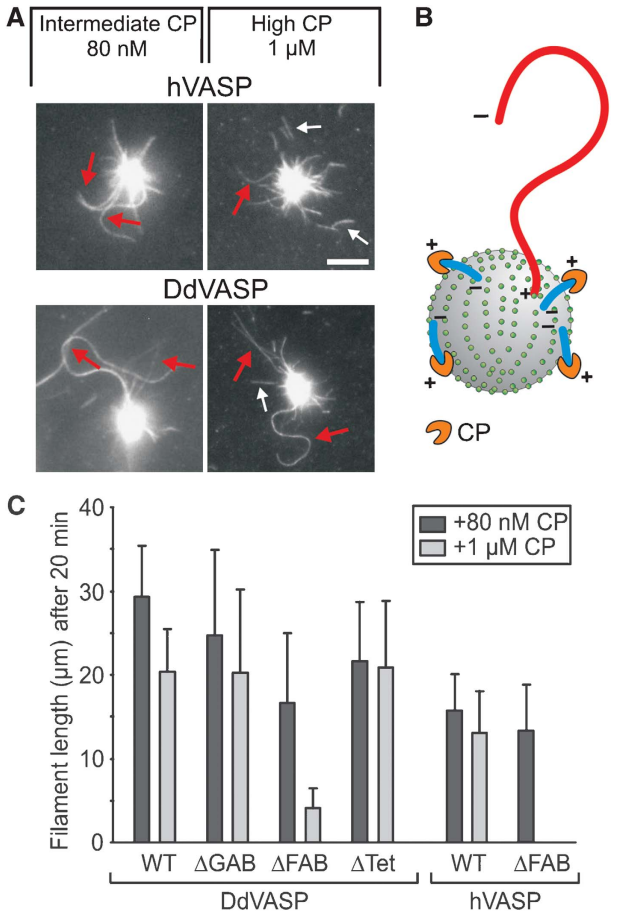

Figure 5 Clustered VASP promotes processive filament elongation in the presence of CP. (**A**) Both human- and DdVASP-coated beads assemble long actin filaments in the presence of up to 1 μM of species-specific CP. Red arrows indicate growing filaments, small white arrows highlight short capped filaments that detached from the beads. Scale bar, 5 μm. (**B**) Scheme illustrating the elimination of filaments growing with their barbed ends pointing away from the bead by CP. Only filaments assembled by VASP at the surface remain. (**C**) The FAB motifs of DdVASP and hVASP are critical for CP resistance upon clustering. For each mutant, the 20% longest filaments growing on coated beads were analysed after 20 min. Mutant hVASPΔFAB failed to produce filaments in the presence of 1 μM CP. For each box, at least 20 filaments were analysed. Data correspond to means ± s.e.m.

In vivo analysis of DdVASP mutants

To test how the different DdVASP mutants contribute to filopodium formation, DdVASP-null cells were used for complementation with GFP-tagged DdVASP constructs. Consistent with a previous report (Han *et al*, 2002), the WT protein accumulated at the leading edge and in filopodia tips. Similarly, subsequent analysis of the reconstituted cells revealed that only DdVASPΔPRD and DdVASPΔGAB could rescue their ability to form filopodia (Figure 6A) and to accumulate at the tips of filopodia and the leading edge (Figure 6B) as shown for DdVASPΔGAB in Supplementary Movie 14. In line with a previous study (Schirenbeck *et al*, 2006), DdVASPΔFAB could barely trigger the formation of filopodia (Figure 6A, Supplementary Movie 15). In these cells, VASPΔFAB also failed to localize to the tip region of the leading edge, but in the few cells that formed short protrusions, an enrichment of the mutant protein was seen

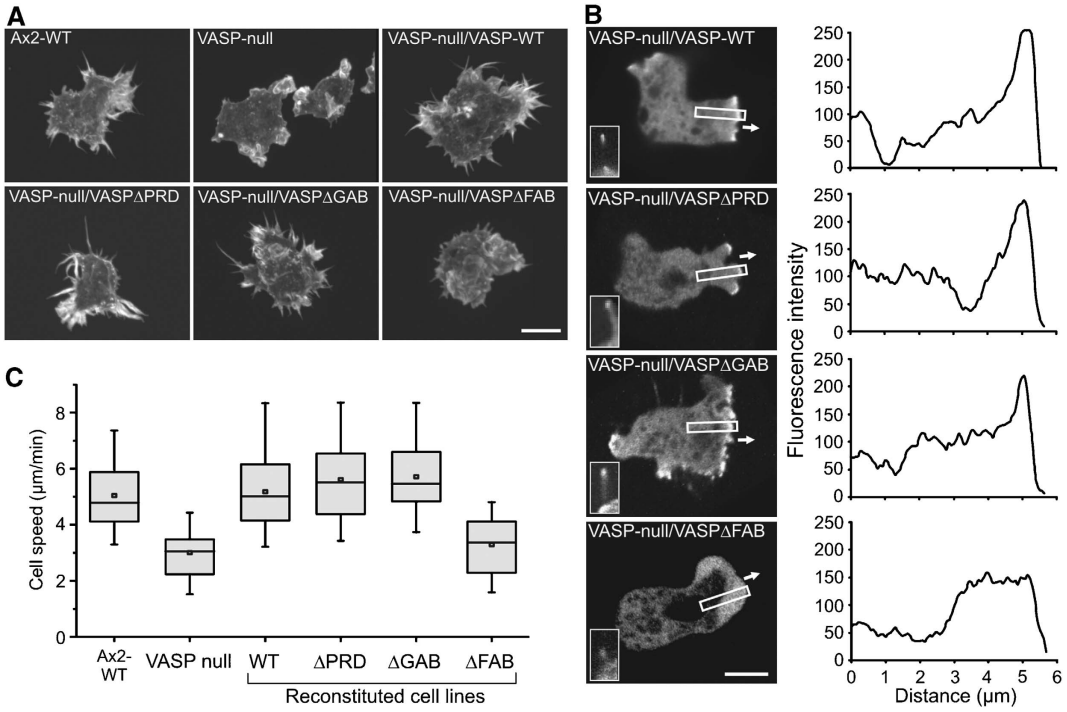

Figure 6 Ability of VASP constructs to restore filopodia formation and cell migration in *Dictyostelium* VASP-null cells. (**A**) 3D reconstitutions of phalloidin-labelled cells indicated are shown. Rescue of filopodia formation was not observed for the VASPΔFAB construct fused to GFP. Typical Ax2-WT and VASP-null cells are shown as controls. Scale bar, 10 μm. (**B**) FAB is critical for VASP targeting to the tip of the leading edge. Confocal sections show accumulation of the indicated GFP-tagged VASP constructs during protrusion of the leading edge, white arrows indicate direction of protrusion during random motility (left panel). Insets show localization of GFP-tagged constructs in filopodia. Intensity profiles corresponding to a linear 8-bit grey scale of the GFP fluorescence in boxed regions are shown (right panel). Scale bar, 10 μm. (**C**) Cell motility of WT, VASP-null and reconstituted cells. Quantification data represent results from three independent experiments. For each cell line, at least 25 cells were analysed. Boxes indicate 25th percentile, median and 75th percentile of all values; error bars indicate 10th and 90th percentile.

(Figure 6B). Unfortunately, and despite multiple attempts, we were not able to generate a cell line expressing reasonable amounts of DdVASPΔTet in the VASP-null mutant for analysis.

In addition to a defect in filopodium formation, DdVASP-null mutants were previously shown to display impaired migratory performance during chemotaxis (Han *et al*, 2002). To examine whether DdVASP contributes to cell motility in general, we monitored cell migration of WT, DdVASP-null and reconstituted cell lines during the growth phase. Motility rates in phosphate buffer were similar for all mutants except for DdVASP-null/DdVASPΔFAB cells that were comparable with VASP-null cells (Figure 6C). These findings indicate that (i) DdVASP-null cells have a general defect in cell motility rather than only a specific defect in chemotaxis and (ii) the FAB motif also has an important role for the function of VASP *in vivo*.

Discussion

F-actin assembly has an important function in protrusion of the plasma membrane during cell migration and the movement of intracellular pathogens (Pollard and Borisy, 2003; Rottner *et al*, 2005; Carlier and Pantaloni, 2007; Pollard, 2007). On the basis of *in vivo* and *in vitro* experiments, VASP has been implicated to promote motility by competing with CP, thus allowing spontaneous actin polymerization at the barbed end (Bear *et al*, 2002; Barzik *et al*, 2005; Pasic *et al*, 2008). Although these findings could also be explained by a direct involvement of VASP in filament elongation, this activity has never been demonstrated. Using TIRF microscopy with purified proteins, we show for the first time that both mammalian and *Dictyostelium* VASP actively drive filament elongation by delivering actin monomers to the growing barbed end. Interestingly, VASP from the highly motile amoeba *Dictyostelium* accelerated filament elongation in our *in vitro* assay as potently as seven-fold. We show that both WH2-domain-related motifs, namely GAB and FAB (Schirenbeck *et al*, 2006; Dominguez, 2007), recruit and deliver actin monomers for efficient filament elongation. The molecular details of VASP-mediated actin assembly uncovered here dispel much of the previous controversy in the field and advance our understanding of the molecular mechanisms of filament attachment to membranes and their elongation in actin-based protrusion during cell motility.

Previously, the PRD region of Ena/VASP proteins was shown to interact with profilin (Reinhard *et al*, 1995a). As profilin–actin complexes constitute the main pool of polymerization-competent actin in eukaryotic cells, these results suggested that, comparable with the proline-rich FH1 domain of formins, the PRD recruits profilin–actin for VASP-mediated actin assembly (Ferron *et al*, 2007). Surprisingly, neither *Dictyostelium* profilins nor human profilin I stimulated VASP-mediated filament elongation in our TIRF assay. VASP and profilin mutants incapable of interacting with the respective partner confirmed this conclusion. These results are, however, consistent with previous studies reporting that VASP enhances the Arp2/3 complex-driven motility of

ActA-coated beads as well as the movement of *Listeria* independent of profilin (Laurent *et al*, 1999; Samarin *et al*, 2003).

On the basis of our findings, we propose that profilin–actin can also bind directly to the GAB (or FAB) for monomer delivery. This hypothesis is in agreement with structural data showing profilin–actin in complex with GAB (Ferron *et al*, 2007) and is further supported by a six-fold higher affinity of GAB of hVASP for profilin–actin than for actin alone (Chereau and Dominguez, 2006). A previous study also found no effect on random cell migration with reconstituted MV^{D7} fibroblasts using a ΔPRD mutant of Mena (Loureiro *et al*, 2002). Taken together, these data suggest that in cells, protein interactions of the proline-rich domain such as recruitment of profilin–actin complexes may be at play only for a subset of Ena/VASP functions.

Our data demonstrate that VASP-mediated actin filament elongation in solution is non-processive. This elongation mechanism thus greatly differs from processive actin assembly by formins under these conditions, which remain associated with the barbed end of one particular growing filament as it elongates (Figure 7A) (Kovar and Pollard, 2004; Romero *et al*, 2004). As a consequence, the elongation rate is independent of the formin concentration (Kovar *et al*, 2006). Our data suggest that VASP-mediated filament elongation in solution follows a mechanism, during which a tetramer attaches to a barbed end, delivers its transiently bound actin subunits and subsequently remains bound to the side of the filament. The strongly impaired elongation rates by the monomeric DdVASPΔTet mutant further suggest that the four polypeptide chains in the tetramer exerts an effect cooperatively, and that accelerated filament elongation is achieved by locally increasing the monomer concentration at the barbed end (Figure 7B). Finally, and in contrast to a recent report (Pasic *et al*, 2008), we did not observe an anti-capping activity of VASP in solution (Figure 3), corroborating our model of a transient interaction of the protein with the barbed end. Although both studies observed an increased filament length in the presence of VASP and CP, we found that this effect is rather due to enhanced filament elongation instead of delayed filament capping by VASP.

The most striking property of VASP is its ability to switch from non-processive actin assembly to processive filament elongation and production of force sufficient to buckle growing filaments upon clustering on a bead. Interestingly, a previous study by Samarin *et al* (2003) showed that whereas hVASP had no effect on actin polymerization stimulated by ActA and Arp2/3 in solution, it significantly enhanced actin assembly when ActA was bound to beads. As clustering of VASP at a surface revealed novel biochemical properties possibly reflecting its mode of action in the cellular context, it was important to understand how processivity is achieved. We show that dense packing on the bead and at least one of the WH2-like domains (GAB or FAB), but surprisingly not the tetramerization of VASP, are required for filament elongation. This finding is in agreement with a previous study, demonstrating that β-thymosin/WH2 domains can promote actin assembly at filament barbed ends when arranged in tandem or inserted in modular proteins (Hertzog *et al*, 2004; Bosch *et al*, 2007). Therefore, we conclude that processive filament elongation and attachment to the surface are not mediated by a single VASP tetramer through a direct-transfer polymerization model (Dickinson and Purich, 2002; Ferron *et al*, 2007), but is rather accomplished by a transient attachment of the growing barbed end to at least two adjacent or a multitude of VASP molecules (Figure 7C), favouring a more flexible mechanism such as the molecular ratchet proposed by Laurent *et al* (1999). This model suggests that propulsion of ActA-coated particles is achieved by cycles of attachment and detachment of VASP to and from actin filaments, enabling insertional incorporation of actin subunits. As shown in Supplementary Figure 2, and consistent with a previous study (Pasic *et al*, 2008), VASP binds barbed ends and subsequently stays attached to the side of the filament while the barbed end continues to grow. Transferring this mode of action to VASP-mediated filament assembly on a surface, it is most likely that VASP stays attached to the side of the filament as it continues to grow by the addition of monomers delivered by other VASP molecules until force-induced detachment occurs (Figure 7C). During these detachment periods, however, the growing filament is constantly tethered to the surface by other VASP molecules. Our model is supported by the strict dependence of filament growth on VASP-density on a bead surface (Figure 4E).

The analyses of the GAB, FAB and Tet motifs revealed additional insights into the mechanism of DdVASP-mediated actin assembly. Unexpectedly, DdVASPΔGAB fully rescued VASP-null *Dictyostelium* cells and also localized properly to the leading edge and the tips of filopodia, the latter of which is consistent with a recent report by Applewhite *et al* (2007), showing that a mutation in GAB does not compromise localization or filopodia formation in MV^{D7} cells, although it led to an increased turnover rate in filopodial tips. Even though beads saturated with DdVASPΔGAB showed a decrease in actin recruitment and a reduced number of processively growing filaments *in vitro* (Figure 4C and D, Supplementary Figure 4C), the relevance of the GAB motif for VASP-mediated actin assembly *in vivo* is currently still unclear. Mutant DdVASPΔFAB also displayed a decrease in actin recruitment but, besides its previously reported lack of bundling activity *in vitro* (Schirenbeck *et al*, 2006, this study), this mutant was unable to rescue VASP-null cells in filopodium formation and cell migration, demonstrating the critical function of the FAB domain. Remarkably, clustered mutant ΔTet showed the same properties in filament elongation and actin recruitment as WT on beads, suggesting that clustering mimics multimerization, which in turn is required to increase interactions with actin filaments. Consistently, tetramerization of VASP was previously shown to be dispensable for *Listeria* motility (Geese *et al*, 2002). It remains to be determined whether and how the cryptic actin-binding site in the C-terminal region of VASP, initially reported by Pasic *et al* (2008), contributes to processive VASP-mediated actin assembly. The effects of the used DdVASP constructs are summarized in Supplementary Table I.

Finally, we also evaluated the contribution of CP on VASP-mediated actin assembly. Although actin filament growth was inhibited by rather low CP concentrations in solution, VASP-mediated actin assembly becomes virtually insensitive even to very high concentrations of CP upon clustering on a bead surface, once more illustrating the profound difference in the biochemical activity of VASP in solution and on beads. The pronounced CP resistance of filament elongation under these conditions argues, however, against the molecular ratchet model of actin-based motility, as this mechanism implies

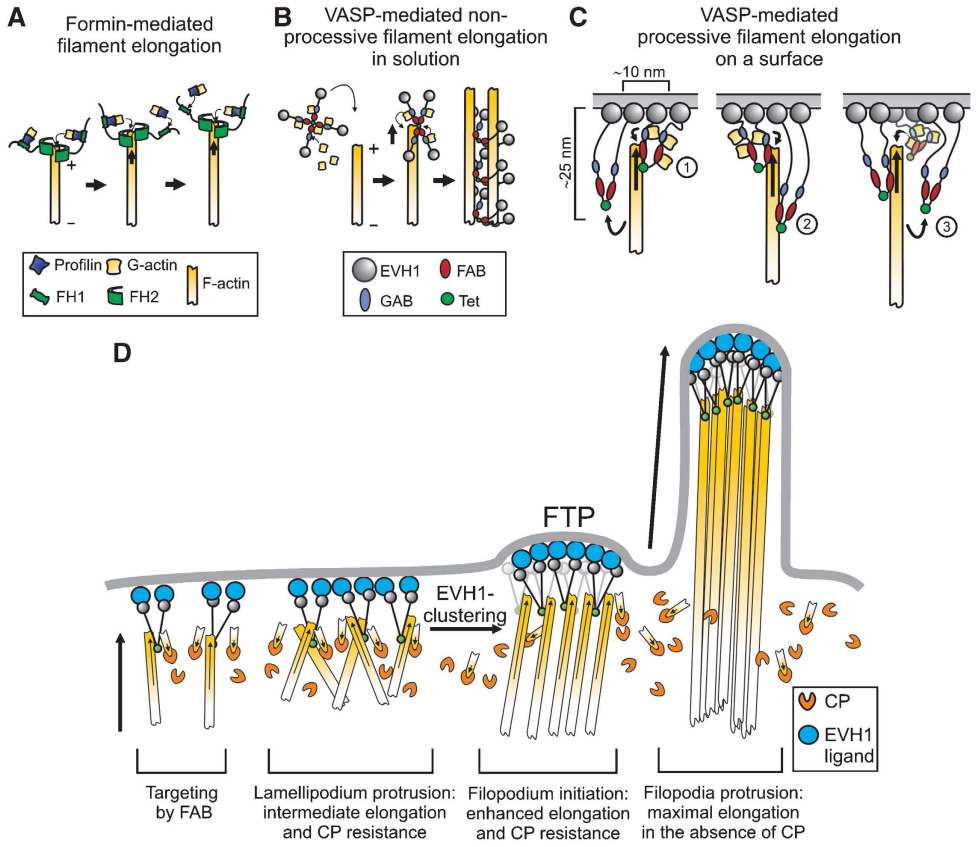

Figure 7 Models of VASP-mediated actin assembly. (**A**) Processive filament elongation by formins is shown for comparison. (**B**) Proposed mechanism for non-processive filament elongation by VASP in solution. VASP tetramers loaded with actin monomers hit a free barbed end, transiently bind and deliver bound actin subunits to it, resulting in non-processive filament elongation. Subsequent side binding of VASP results in decoration of the filament and mediates bundle formation. (**C**) Proposed mechanism for processive filament elongation on a surface: (1) VASP tetramers tethered to the surface bind to actin and deliver monomers through their WH2 domains to the barbed end. (2) After delivery, VASP remains bound to the side of the filament as the barbed end elongates in response to the delivery of actin monomers by other VASP molecules. Owing to its flexible architecture, VASP may stay attached to the side of the filament up to 20–30 nm away from the surface. (3) Stretched VASP molecules eventually detach from the filament due to continuous elongation of the barbed end and are afterwards available for a new cycle of actin addition. During the detachment period, the growing filament is constantly tethered to the surface by other VASP molecules. Decoration of the barbed end region by multiple VASP molecules is presumed to prevent access of CP to the filament barbed end. As filament-growth-induced detachment of VASP does not occur in solution, processive elongation can be accomplished only on a surface. (**D**) Functions of VASP in cell protrusions. VASP molecules docked on the membrane through their EVH1 domains anchor actin filaments through their WH2 domains. This anchorage may in turn stabilize the localization of VASP to the membrane. Clustering of VASP allows lamellipodium protrusion in the presence of CP, which itself might serve to eliminate unproductive filaments. Stronger clustering mediated by an EVH1 ligand may trigger the formation of the filopodium tip complex (FTP), allowing the transition from lamellipodium to filopodium formation. For the sake of simplicity, VASP is illustrated only as a dimer in C and D.

filament capping during the detachment periods and hence excludes the formation of long filaments (Laurent *et al*, 1999). Thus, the mechanism used by VASP seems to combine properties of both the rigid direct-transfer polymerization model that supports an active involvement of VASP in monomer incorporation into the growing barbed end (Mogilner and Oster, 2003) and the molecular ratchet in which a transient interaction of a single VASP tetramer with the filament was postulated. Furthermore, as in the presence of CP only appropriately oriented filaments are supposed to grow, it is conceivable that in addition to the assumed function of CP *in vivo* in maintaining a large pool of polymerizable actin and generating capped short and stiff filaments embedded in the lamellipodial network to push the membrane forward (Carlier *et al*, 2003; Pollard and Borisy, 2003), CP could be used to eliminate the growth of wrongly oriented filaments in the leading edge (Figure 7D). Consistently, a recent study showed a restriction of CP only to the tip of the lamellipodium in B16F1 cells but not to the lamellipodial actin meshwork, leading to a similar conclusion (Lai *et al*, 2008). Thus, CP might be required to establish a well-regulated lamellipodial architecture with the filament barbed ends pointing towards the membrane sufficiently tethered for directed protrusion (Koestler *et al*, 2008).

Interestingly, the only mutants that failed to processively elongate long filaments at higher CP concentrations were both human and *Dictyostelium* ΔFAB proteins, suggesting that the lower CP resistance may result from an augmented access of CP to the growing barbed ends. Therefore, differential sensitivity to the presence of CP rather than lack of bundling activity (Schirenbeck *et al*, 2006) might explain the inability of this DdVASP mutant to rescue filopodia formation and motility in VASP-null cells. Both the inability of DdVASPΔFAB to resist CP on the bead surface and its failure to localize to the protruding leading edge may arise from a weaker interaction of elongating filaments with

DdVASPΔFAB. A previous study indeed demonstrated that the WH2 domain of N-WASP mediates filament barbed-end capture to membranes even in the presence of CP (Co *et al*, 2007), suggesting that the WH2 domain of N-WASP and the FAB motif of VASP may share similar properties. However, and in agreement with its *in vitro* activity, mammalian VASPΔFAB increased *Listeria* motility (Geese *et al*, 2002), suggesting that, in contrast to the lamellipodium tip where CP is enriched, the CP concentration in the cytosol is sufficiently low to allow tethering of this VASP mutant to the growing comet tail. Although the CP concentration at the *Listeria* surface is not known, reconstituted *Listeria* motility with purified proteins revealed an optimal CP concentration of 50 nM (Loisel *et al*, 1999), a concentration that still allows fast and processive actin filament growth with the ΔFAB mutants in our *in vitro* assay.

Taken together, our observations suggest that localization of DdVASP to the leading edge and to sites of filopodium formation are regulated differently. Although the FAB mutant failed to robustly localize to the front of the leading edge, it still showed accumulation in the tips of the few short filopodia that were still formed. Thus, filopodium initiation appears to require strong clustering of VASP, presumably triggered by clustering of the EVH1 ligand at the plasma membrane resulting in maximal protrusion (Figure 7D). This hypothesis is consistent with the direct correlation between VASP density and the protrusion rate in B16 melanoma cells (Rottner *et al*, 1999).

Materials and methods

Protein expression and purification

The DNA constructs used and the purification of proteins are described in the Supplementary data.

TIRF microscopy

Time-lapse evanescent wave fluorescence microscopy was essentially performed as described (Kovar and Pollard, 2004; Kuhn and Pollard, 2005), with the exemption that G-actin was labelled on Cys-374 with Alexa-Fluor-488-C_5-maleimide (Molecular Probes, Cambridge, UK). All proteins to be analysed were premixed in TIRF buffer and subsequently added to G-actin. Images from an Olympus IX-81 inverted microscope were captured every 10 or 15 s with exposures of 200 or 500 ms with a Hamamatsu ER C8484 CCD camera (Hamamatsu Corp., Bridgewater, NJ). The pixel size corresponded to 0.11 μm.

The elongation rates of filaments were calculated with ImageJ software using the plugins MtrackJ and Manual Tracking. Each experiment was repeated at least three times. For each polymerization measurement, at least 15 barbed ends of individual filaments were manually tracked. In case of filaments growing on beads, the total length of the filament was measured for every time frame. Filament growth rates were diagrammed as plots of length versus time and the average elongation rate in subunits per second was calculated from linear regressions of the slopes. The increase of fluorescence intensity of VASP-coated beads was determined from 12-bit time-lapse series micrographs using the Time Series Analyzer plugin from ImageJ. As the GST tag did not affect the properties of the VASP constructs in the TIRF assay but improved solubility, it was not cleaved off except stated otherwise.

Electron microscopy

Purified untagged mVASP and mVASPΔ118–304 (each 0.7 mg/ml) were diluted 1:40 to 1:80 in spraying buffer (100 mM ammonium acetate, pH 7.3, 30% glycerol). Replicas were produced essentially as described previously (Aebi and Baschong, 2006). Micrographs were acquired on an FEI Morgagni TEM and measurements were performed with ImageJ.

Supplementary data

Supplementary data are available at *The EMBO Journal* Online (http://www.embojournal.org).

Acknowledgements

We thank A Breskott, L Litz and M Brandstetter for excellent technical assistance, I Chizhov and G Tsiavaliaris for support, DJ Manstein for infrastructure, the confocal imaging facility of the Hannover Medical School, and M Schleicher for anti-Cap32/34 antibodies. We also thank K Rottner and TEB Stradal for helpful discussions and critical reading of the manuscript. This work was supported by a grant to JF (FA 330/4-1) from the Deutsche Forschungsgemeinschaft. GPR and JVS acknowledge the support of the City of Vienna/Zentrum fuer Innovation und Technologie through the Spot of Excellence grant 'Center of Molecular and Cellular Nanostructure'.

References

Aebi U, Baschong W (2006) Glycerol spraying/low-angle rotary metal shadowing. In *Cell Biology—A Laboratory Handbook*, J Celis (ed), 3rd ed, pp 241–246. London: Elsevier

Applewhite DA, Barzik M, Kojima S, Svitkina TM, Gertler FB, Borisy GG (2007) Ena/VASP proteins have an anti-capping independent function in filopodia formation. *Mol Biol Cell* **18:** 2579–2591

Bachmann C, Fischer L, Walter U, Reinhard M (1999) The EVH2 domain of the vasodilator-stimulated phosphoprotein mediates tetramerization, F-actin binding, and actin bundle formation. *J Biol Chem* **274:** 23549–23557

Ball LJ, Kuhne R, Hoffmann B, Hafner A, Schmieder P, Volkmer-Engert R, Hof M, Wahl M, Schneider-Mergener J, Walter U, Oschkinat H, Jarchau T (2000) Dual epitope recognition by the VASP EVH1 domain modulates polyproline ligand specificity and binding affinity. *EMBO J* **19:** 4903–4914

Barzik M, Kotova TI, Higgs HN, Hazelwood L, Hanein D, Gertler FB, Schafer DA (2005) Ena/VASP proteins enhance actin polymerization in the presence of barbed end capping proteins. *J Biol Chem* **280:** 28653–28662

Bear JE, Svitkina TM, Krause M, Schafer DA, Loureiro JJ, Strasser GA, Maly IV, Chaga OY, Cooper JA, Borisy GG, Gertler FB (2002) Antagonism between Ena/VASP proteins and actin filament capping regulates fibroblast motility. *Cell* **109:** 509–521

Bosch M, Le KH, Bugyi B, Correia JJ, Renault L, Carlier MF (2007) Analysis of the function of Spire in actin assembly and its synergy with formin and profilin. *Mol Cell* **28:** 555–568

Brindle NP, Holt MR, Davies JE, Price CJ, Critchley DR (1996) The focal-adhesion vasodilator-stimulated phosphoprotein (VASP) binds to the proline-rich domain in vinculin. *Biochem J* **318:** 753–757

Carlier MF, Le Clainche C, Wiesner S, Pantaloni D (2003) Actin-based motility: from molecules to movement. *Bioessays* **25:** 336–345

Carlier MF, Pantaloni D (2007) Control of actin assembly dynamics in cell motility. *J Biol Chem* **282:** 23005–23009

Chereau D, Dominguez R (2006) Understanding the role of the G-actin-binding domain of Ena/VASP in actin assembly. *J Struct Biol* **155:** 195–201

Co C, Wong DT, Gierke S, Chang V, Taunton J (2007) Mechanism of actin network attachment to moving membranes: barbed end capture by N-WASP WH2 domains. *Cell* **128:** 901–913

Dent EW, Kwiatkowski AV, Mebane LM, Philippar U, Barzik M, Rubinson DA, Gupton S, Van Veen JE, Furman C, Zhang J, Alberts AS, Mori S, Gertler FB (2007) Filopodia are required for cortical neurite initiation. *Nat Cell Biol* **9:** 1347–1359

Dickinson RB, Purich DL (2002) Clamped-filament elongation model for actin-based motors. *Biophys J* **2:** 605–617

Dominguez R (2007) The beta-thymosin/WH2 fold: multifunctionality and structure. *Ann N Y Acad Sci* **1112:** 86–94

Ferron F, Rebowski G, Lee SH, Dominguez R (2007) Structural basis for the recruitment of profilin–actin complexes during filament elongation by Ena/VASP. *EMBO J* **26:** 4597–4606

Geese M, Loureiro JJ, Bear JE, Wehland J, Gertler FB, Sechi AS (2002) Contribution of Ena/VASP proteins to intracellular motility of *Listeria* requires phosphorylation and proline-rich core but not F-actin binding or multimerization. *Mol Biol Cell* **13:** 2383–2396

Gertler FB, Niebuhr K, Reinhard M, Wehland J, Soriano P (1996) Mena, a relative of VASP and *Drosophila* enabled, is implicated in the control of microfilament dynamics. *Cell* **87:** 227–239

Han YH, Chung CY, Wessels D, Stephens S, Titus MA, Soll DR, Firtel RA (2002) Requirement of a vasodilator-stimulated phosphoprotein family member for cell adhesion, the formation of filopodia, and chemotaxis in *Dictyostelium*. *J Biol Chem* **277:** 49877–49887

Hertzog M, van Heijenoort C, Didry D, Gaudier M, Coutant J, Gigant B, Didelot G, Préat T, Knossow M, Guittet E, Carlier MF (2004) The beta-thymosin/WH2 domain; structural basis for the switch from inhibition to promotion of actin assembly. *Cell* **117:** 611–623

Jenzora A, Behrendt B, Small JV, Wehland J, Stradal TE (2005) PREL1 provides a link from Ras signalling to the actin cytoskeleton via Ena/VASP proteins. *FEBS Lett* **580:** 455–463

Koestler SA, Auinger S, Vinzenz M, Rottner K, Small JV (2008) Differentially oriented populations of actin filaments generated in lamellipodia collaborate in pushing and pausing at the cell front. *Nat Cell Biol* **10:** 306–313

Kovar DR, Harris ES, Mahaffy R, Higgs HN, Pollard TD (2006) Control of the assembly of ATP- and ADP-actin by formins and profilin. *Cell* **124:** 423–435

Kovar DR, Pollard TD (2004) Insertional assembly of actin filament barbed ends in association with formins produces piconewton forces. *Proc Natl Acad Sci USA* **101:** 14725–14730

Krause M, Leslie JD, Stewart M, Lafuente EM, Valderrama F, Jagannathan R, Strasser GA, Rubinson DA, Liu H, Way M, Yaffe MB, Boussiotis VA, Gertler FB (2004) Lamellipodin, an Ena/VASP ligand, is implicated in the regulation of lamellipodial dynamics. *Dev Cell* **7:** 571–583

Kuhn JR, Pollard TD (2005) Real-time measurements of actin filament polymerization by total internal reflection fluorescence microscopy. *Biophys J* **88:** 1387–1402

Kursula P, Kursula I, Massimi M, Song YH, Downer J, Stanley WA, Witke W, Wilmanns M (2008) High-resolution structural analysis of mammalian profilin 2a complex formation with two physiological ligands: the formin homology 1 domain of mDia1 and the proline-rich domain of VASP. *J Mol Biol* **375:** 270–290

Kwiatkowski AV, Rubinson DA, Dent EW, Edward van Veen J, Leslie JD, Zhang J, Mebane LM, Philippar U, Pinheiro EM, Burds AA, Bronson RT, Mori S, Fässler R, Gertler FB (2007) Ena/VASP is required for neuritogenesis in the developing cortex. *Neuron* **56:** 441–455

Lafuente EM, van Puijenbroek AA, Krause M, Carman CV, Freeman GJ, Berezovskaya A, Constantine E, Springer TA, Gertler FB, Boussiotis VA (2004) RIAM, an Ena/VASP and Profilin ligand, interacts with Rap1-GTP and mediates Rap1-induced adhesion. *Dev Cell* **7:** 585–595

Lai APL, Szczodrak M, Block J, Faix J, Breitsprecher D, Mannherz HG, Stradal TE, Dunn GA, Small JV, Rottner K (2008) Arp2/3-complex interactions and actin network turnover in lamellipodia. *EMBO J* **27:** 982–992

Lambrechts A, Kwiatkowski AV, Lanier LM, Bear JE, Vandekerckhove J, Ampe C, Gertler FB (2000) cAMP-dependent protein kinase phosphorylation of EVL, a Mena/VASP relative, regulates its interaction with actin and SH3 domains. *J Biol Chem* **275:** 36143–36151

Laurent V, Loisel TP, Harbeck B, Wehman A, Grobe L, Jockusch BM, Wehland J, Gertler FB, Carlier MF (1999) Role of proteins of the Ena/VASP family in actin-based motility of *Listeria* monocytogenes. *J Cell Biol* **144:** 1245–1258

Loisel TP, Boujemaa R, Pantaloni D, Carlier MF (1999) Reconstitution of actin-based motility of *Listeria* and *Shigella* using pure proteins. *Nature* **401:** 613–616

Loureiro JJ, Rubinson DA, Bear JE, Baltus GA, Kwiatkowski AV, Gertler FB (2002) Critical roles of phosphorylation and actin binding motifs, but not the central proline-rich region, for Ena/vasodilator-stimulated phosphoprotein (VASP) function during cell migration. *Mol Biol Cell* **13:** 2533–2546

Mogilner A, Oster G (2003) Force generation by actin polymerization II: the elastic ratchet and tethered filaments. *Biophys J* **84:** 1591–1605

Niebuhr K, Ebel F, Frank R, Reinhard M, Domann E, Carl UD, Walter U, Gertler FB, Wehland J, Chakraborty T (1997) A novel proline-rich motif present in ActA of *Listeria* monocytogenes and cytoskeletal proteins is the ligand for the EVH1 domain, a protein module present in the Ena/VASP family. *EMBO J* **16:** 5433–5444

Pasic L, Kotova TI, Schafer DA (2008) Ena/VASP proteins capture actin filament barbed ends. *J Biol Chem* **283:** 9814–9819

Paunola E, Mattila PK, Lappalainen P (2002) WH2 domain: a small, versatile adapter for actin monomers. *FEBS Lett* **513:** 92–97

Pollard TD (2007) Regulation of actin filament assembly by Arp2/3 complex and formins. *Annu Rev Biophys Biomol Struct* **36:** 451–477

Pollard TD, Borisy GG (2003) Cellular motility driven by assembly and disassembly of actin filaments. *Cell* **112:** 453–465

Reinhard M, Giehl K, Abel K, Haffner C, Jarchau T, Hoppe V, Jockusch BM, Walter U (1995a) The proline-rich focal adhesion and microfilament protein VASP is a ligand for profilins. *EMBO J* **14:** 1583–1589

Reinhard M, Halbrugge M, Scheer U, Wiegand C, Jockusch BM, Walter U (1992) The 46/50 kDa phosphoprotein VASP purified from human platelets is a novel protein associated with actin filaments and focal contacts. *EMBO J* **11:** 2063–2070

Reinhard M, Jouvenal K, Tripier D, Walter U (1995b) Identification, purification, and characterization of a zyxin-related protein that binds the focal adhesion and microfilament protein VASP (vasodilator-stimulated phosphoprotein). *Proc Natl Acad Sci USA* **92:** 7956–7960

Romero S, Le Clainche C, Didry D, Egile C, Pantaloni D, Carlier MF (2004) Formin is a processive motor that requires profilin to accelerate actin assembly and associated ATP hydrolysis. *Cell* **119:** 419–429

Rottner K, Behrendt B, Small JV, Wehland J (1999) VASP dynamics during lamellipodia protrusion. *Nat Cell Biol* **1:** 321–322

Rottner K, Stradal TE, Wehland J (2005) Bacteria–host-cell interactions at the plasma membrane: stories on actin cytoskeleton subversion. *Dev Cell* **9:** 3–17

Samarin S, Romero S, Kocks C, Didry D, Pantaloni D, Carlier MF (2003) How VASP enhances actin-based motility. *J Cell Biol* **163:** 131–142

Schirenbeck A, Arasada R, Bretschneider T, Stradal TE, Schleicher M, Faix J (2006) The bundling activity of vasodilator-stimulated phosphoprotein is required for filopodium formation. *Proc Natl Acad Sci USA* **103:** 7694–7699

Svitkina TM, Bulanova EA, Chaga OY, Vignjevic DM, Kojima S, Vasiliev JM, Borisy GG (2003) Mechanism of filopodia initiation by reorganization of a dendritic network. *J Cell Biol* **160:** 409–421

Trichet L, Sykes C, Plastino J (2008) Relaxing the actin cytoskeleton for adhesion and movement with Ena/VASP. *J Cell Biol* **181:** 19–25

Watanabe N, Madaule P, Reid T, Ishizaki T, Watanabe G, Kakizuka A, Saito Y, Nakao K, Jockusch BM, Narumiya S (1997) p140mDia, a mammalian homolog of *Drosophila* diaphanous, is a target protein for Rho small GTPase and is a ligand for profilin. *EMBO J* **16:** 3044–3056

